

Introduction

The origin, thickness and composition of the crust of Mars remain important research topics. Understanding how the crust was formed first requires to constrain the composition of the primary melts extracted from the mantle. This can be done either experimentally or through modeling. Because experiments are time-consuming and resource-intensive, modeling tools are desirable to explore how mantle sources of various composition can melt over a range of P-T conditions. We have recently developed a new melting model [1], MAGMARS, specifically designed to simulate the melting of FeO-rich peridotite—and the Martian mantle in particular—using the growing number of relevant experimental studies now available.

In the publication introducing MAGMARS [1], we applied the model to the Adirondack-class basalts analyzed at Gusev crater by Spirit, the most widely accepted example of Martian primitive basalt [2-4]. Here, we review some other candidates of primitive Martian basalts that could have largely escaped igneous differentiation and therefore represent snapshots of the melting conditions in the mantle. While the number of possible primitive basalts sampled by meteorites and analyzed by rovers is still limited, they are characterized by contrasting crystallization ages and have the potential to highlight how the mantle composition and thermal state evolved through time.

The MAGMARS melting model

The MAGMARS melting model follows the same overall approach as the Kinzler and Grove (1992) [5] family of models. Melting equations and partition coefficients are used to calculate the concentration of minor and/or incompatible elements (Al_2O_3 , Na_2O , K_2O , TiO_2 , P_2O_5) that are then used to lower the variance of the system and determine the concentration of major elements (FeO , MgO , CaO , SiO_2) with polynomial regressions.

MAGMARS can be used in isobaric mode for direct comparison with the experimental calibration database and other melting models (Fig. 1).

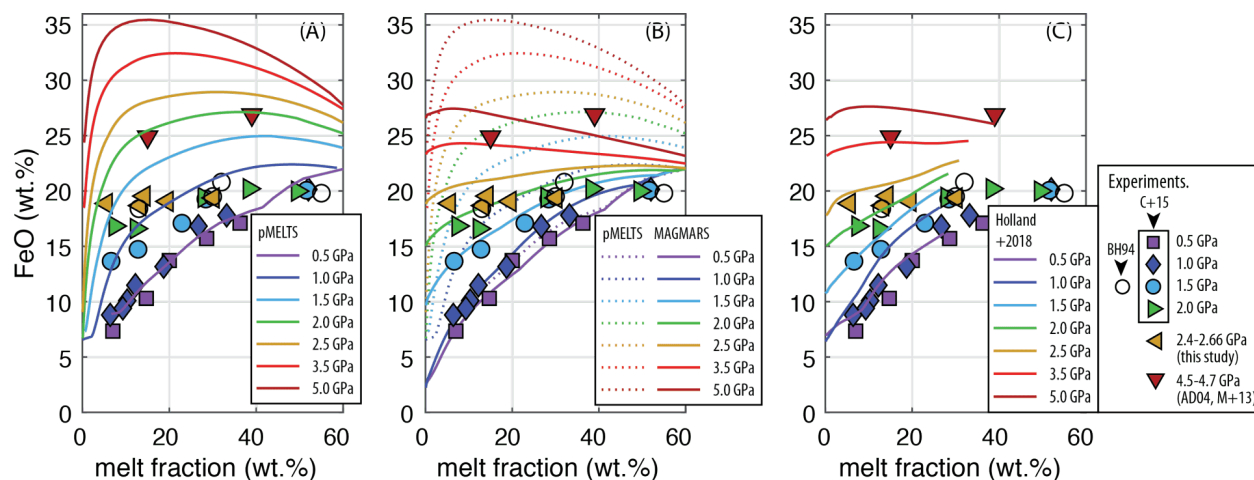


Fig. 1. FeO content of experiments [1, 6-9] compared to modelled primary melts with (A) pMELTS [10], (B) MAGMARS [1] and (C) Perple_X [11] using the solutions models of [12] as a function of the total melt fraction. Note that pMELTS systematically overestimates the FeO

content while MAGMARS and Perple_X predict the experimental FeO content accurately. Figure reproduced from [1].

Here we use MAGMARS in near-fractional polybaric mode to constrain the source composition and P-T conditions of Martian primitive basalts as melt extraction is believed to be highly efficient during decompression melting. The solidus temperature of each mantle source is calculated from the composition of the first 0.1 % melt produced at the pressure of interest using an empirical liquid-thermometer [1]. The pressure is then progressively lowered until the mantle adiabat intersects the solidus. Once melting has started, the melt is continuously extracted and the mantle composition updated. The final melt composition is calculated by adding all the melt increments produced at different depth in one "pooled" aggregate melt composition (Fig. 2).

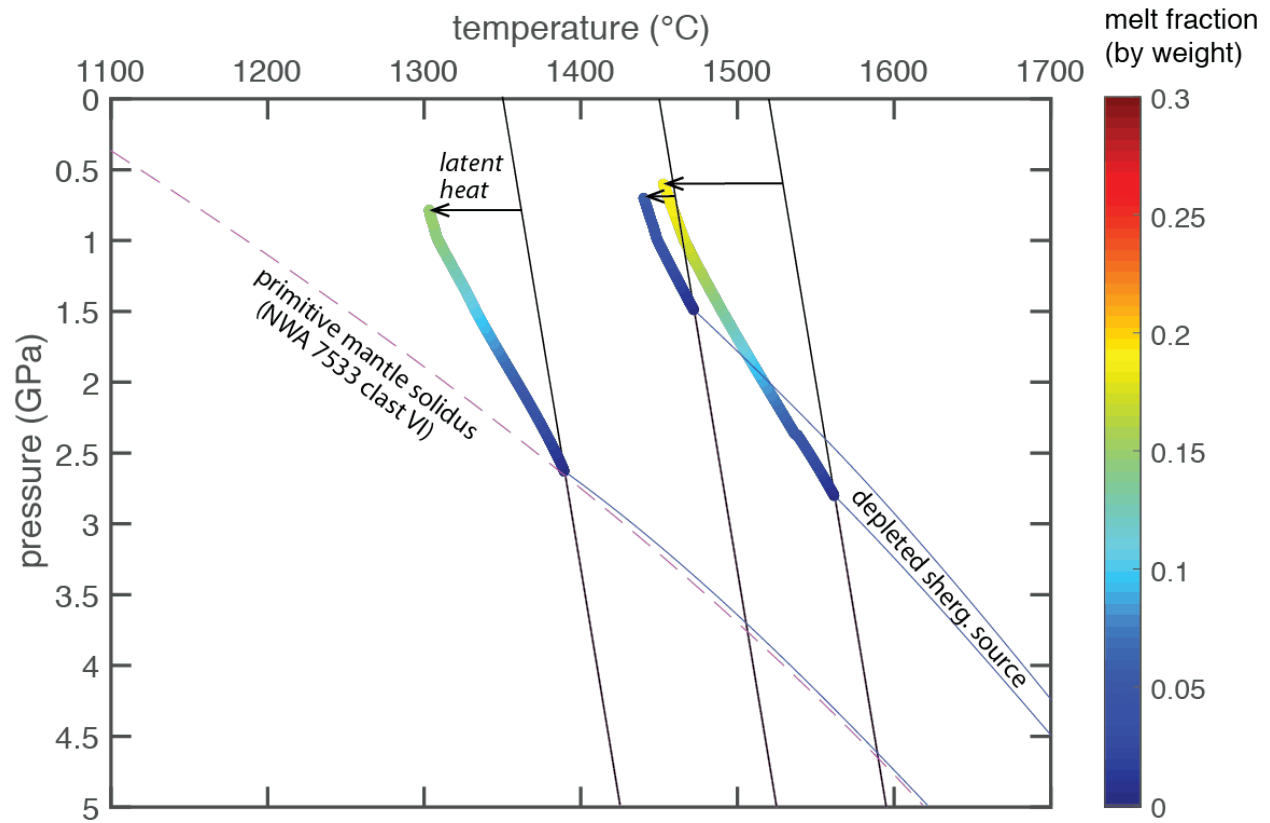


Fig. 2. Near-fractional polybaric melting paths for two different mantle sources (primitive mantle and possible source of the depleted shergottites) along 3 mantle adiabats (1350, 1450 and 1520 °C). The solid blue lines represent the solidi calculated with MAGMARS. The dashed magenta line is the parametrized solidus of [6]. The color map indicates the total amount of melting. The composition of the aggregate melts corresponds to the composition of clast VI in NWA 7533 [13] or the depleted shergottite Yamato 980459 [14] after minor olivine fractionation (0-10 %), see next section.

Mantle source compositions

The mantle sources of the following melt compositions ($\pm 0\text{-}10\%$ olivine fractionation) were constrained with MAGMARS:

NWA 7034/7533: regolith breccias possibly representative of the primary Martian crust, formed within 100 Myr of Mars' accretion. They contain basaltic clasts that could represent near-primary melts [13,15]. We constrain the formation of the mantle melts parental to a vitrophyre [15] and clast VI in NWA 7533 [13].

Adirondack basalts: analyzed by the Spirit rover at Gusev crater. Most likely derived from a depleted mantle with low alkali content, used as case study in [1].

Columbia Hills basalts: also analyzed by the Spirit rover at Gusev crater. Compared to the Adirondack-class basalts, they are much richer in alkali elements. We constrained the mantle sources of the samples Humble Peak, Ace, Stars, Fastball and Irvine.

Nakhlites-chassignites: the parental melt possibly common to nakhlites and chassignites is taken from [16], reconstructed from melt inclusions in the chassignite NWA 2737.

Depleted shergottites: the meteorite Yamato 980459 [14] is assumed to represent a primary mantle melt in equilibrium with a FeO-poor mantle source containing olivine Fo_{85} .

Enriched shergottites: following [17], we assume that the primary melt parental to enriched shergottites correspond to the bulk composition of LAR 06319 and was in equilibrium with olivine Fo_{80} [18].

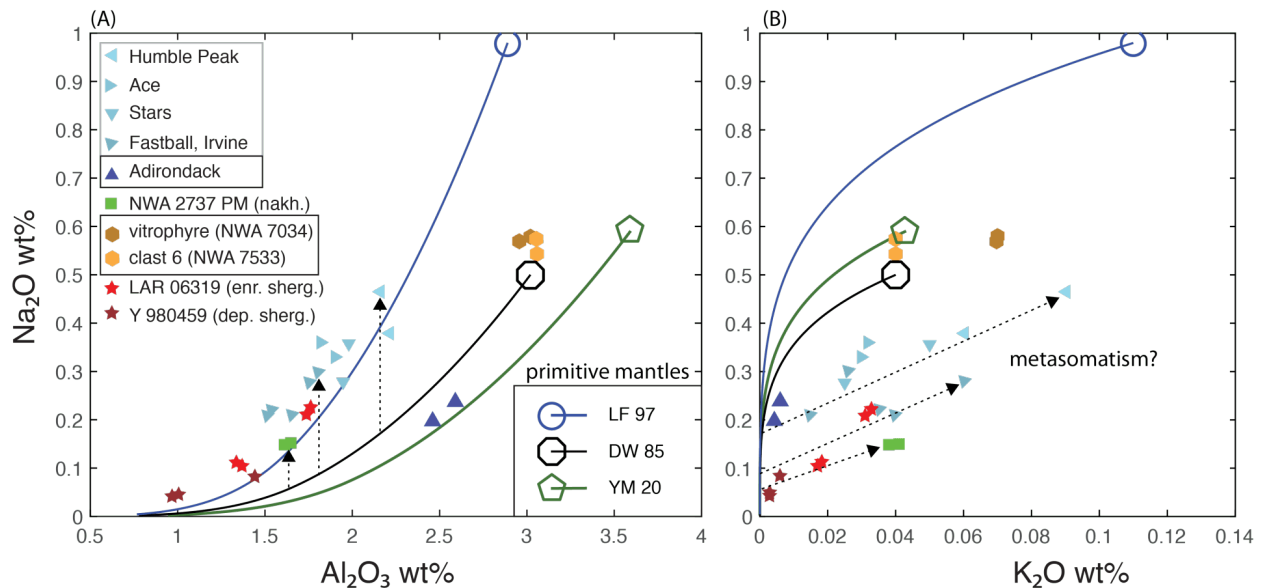


Fig.3. Concentration of incompatible elements in the different mantle sources. In some cases, several mantle sources were found for the same sample as reconstructing the mantle source with MAGMARS can lead to non-unique results. For example, a highly depleted (i.e. refractory) mantle that melts to a small extent can produce liquids nearly identical to the ones produced by

a more fertile mantle melting to a greater extent (Fig. 2, depleted shergottites). The solid lines represent the trajectory of residual mantle compositions when melting the model Martian mantles of [19-21]. The primitive mantle compositions are represented by the corresponding open symbol. The mantle source of NWA 7034/7533 could be nearly identical to the primitive DW 85 mantle and is the only studied sample that could derive from a primitive mantle. The source of the Adirondack basalts could be equivalent to a depleted DW 85 or YM 20 mantle (solution exists for both associated Mg#, 75 vs 79). All other mantle sources are enriched in alkalis compared to DW 85 and YM 20 residual mantles. In (A), mantle sources of the Columbia Hills basalts, chassignites and enriched shergottites seem to align on the trajectory of LF 97 residual mantles. However, in (B), compared to this trajectory, these mantle sources are shown to be enriched in K₂O. The high K₂O content could result from the re-fertilization of depleted to highly depleted mantle sources by fluids and melts (metasomatism; dotted arrows).

Table 1. Average composition and P-T conditions of mantle sources as calculated with MAGMARS, organized by decreasing age of crystallization of the different samples.

	primitive		mantle sources of martian magmas				
	DW85	NWA 7034	Adirondack	Columbia Hills	nakh-chas	dep. sherg.	enr. sherg.
SiO ₂	44.4	44.4	45.5	44.9	45.4	45.7	45.7
TiO ₂	0.13	0.24	0.07	0.12	0.25	0.08	0.09
Al ₂ O ₃	3.02	3.02	2.52	1.84	1.63	1.14	1.55
Cr ₂ O ₃	0.76	0.77	0.92	0.84	0.77	0.91	0.90
FeO	17.9	17.1	17.0	17.2	16.9	12.5	15.9
MnO	0.46	0.47	0.47	0.47	0.47	0.48	0.47
MgO	30.2	30.8	31.7	32.7	33.3	37.8	33.7
CaO	2.44	2.41	1.59	1.22	1.13	1.24	1.46
Na ₂ O	0.50	0.57	0.22	0.31	0.15	0.06	0.16
K ₂ O	0.04	0.055	0.005	0.04	0.04	0.004	0.02
P ₂ O ₅	0.16	0.14	0.05	0.10	0.02	0.04	0.05
<i>T_p</i> (°C)		1350–1500	1390–1440	1360–1440	1400–1450	1460–1520	1440–1480
<i>P</i> (GPa)		1.5–2.0	1.7–2.1	1.2–1.8	1.2–1.6	1.2–1.6	1.6–2.0
Age (Ga)		4.4	3.7	3.7	1.3	0.5	0.2

Implications: All but the oldest sampled mantle sources (NWA 7034/7533) are depleted (i.e. refractory), which suggest that they had been affected by prior events of melting. This is consistent with the early and rapid formation of the crust during the Pre-Noachian. All mantle sources sampled afterwards could have been altered by the early crust-mantle differentiation event.

Mantle potential temperatures (T_p)

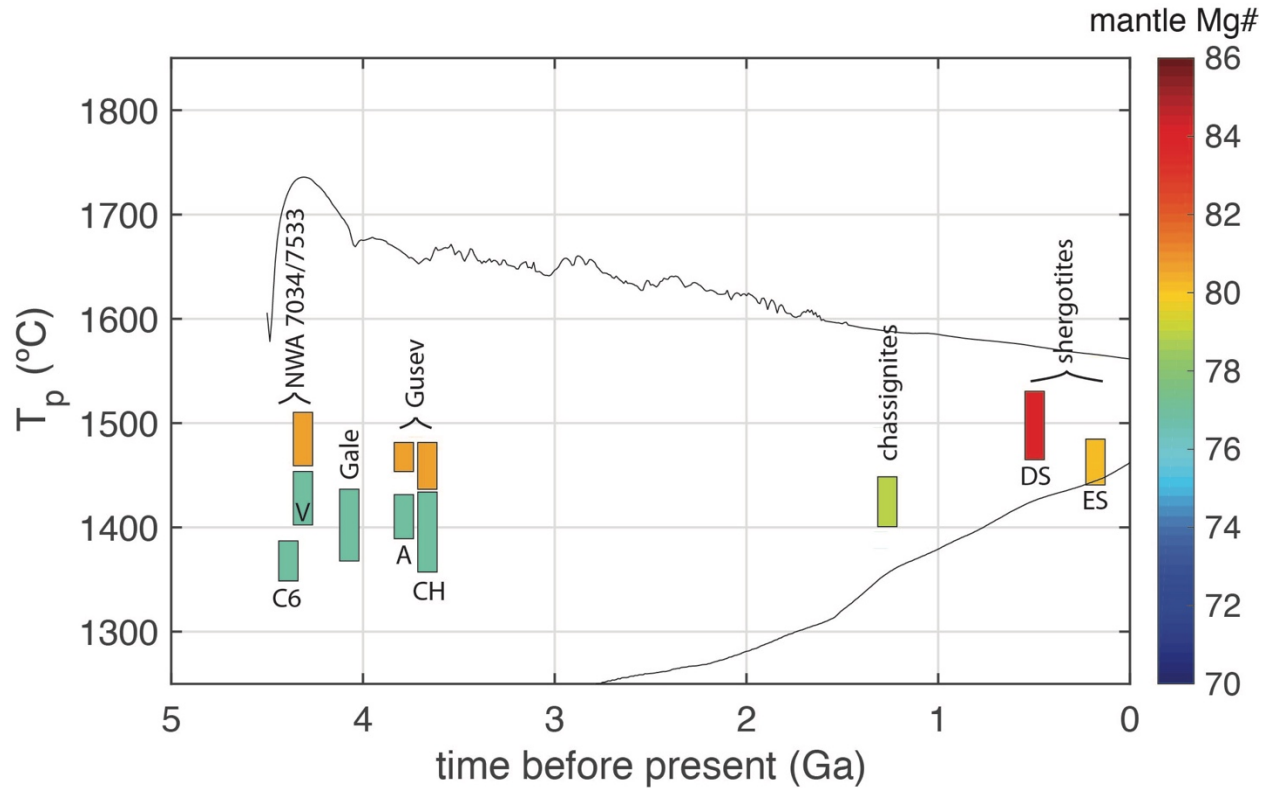


Fig. 4. Mantle potential temperature of the studied primary Martian melts as a function of their approximate crystallization age. C6 = clast VI [16]. V = vitrophyre [17], A = Adirondack-class basalts, CH = Columbia Hills basalts, DS = depleted shergottites, ES = enriched shergottites. For NWA 7045/7533 and Gusev crater basalts, we tested the influence of varying the Mg# of the source (color map). For any sample, if the Mg# of the source was higher than what is assumed here, the parental melt would be more mafic (MgO rich) and the T_p should be shifted upward by ~ 50 °C per 3 Mg# unit. All T_p estimates also assume that melting is near-fractional polybaric (see methods). If melting was instead closer to batch melting, the T_p should also be slightly higher (by 10-40 °C, depending on the sample). With these assumptions, the displayed T_p likely represent lower limits. The solid lines represent the minimum and maximum T_p of the melting zone in a global thermo-chemical evolution model of Mars (thick crust model of ~ 60 km on average) [22]. The range of T_p is pinched towards the present due to the secular cooling of the mantle (lower maximum T_p), increased lithosphere thickness and increasingly depleted nature of the mantle (higher minimum T_p).

Implications: The T_p of sampled primitive basalts seem to have remained relatively stable. This could seem surprising considering that the planet has significantly cooled over the past 4.56+ billion years. However, several bias should be considered. First, melts produced at very high temperature on Mars would have been extremely FeO rich (~ 25 wt.%; Fig. 1) and dense. It is therefore possible that the hottest primary melts from the Pre-Noachian/Noachian were not sampled because they never reached the surface, at least not until substantial igneous differentiation could take place. Second, the mantle affected by partial melting in recent history is not representative of the bulk mantle. Melting is believed to have been extremely localized over the past billion year (e.g. Tharsis, Elysium) and the mantle at these locations (the possible

source of shergottites) undeniably represents the hottest regions of the Martian mantle. Overall, the sampled primary melts, while not fully representative, seem to be in line with global thermal evolution models.

- [1] Collinet, M., Plesa, A.-C., Grove, T. L., Schwinger, S., Ruedas, T., & Breuer, D. (2021). MAGMARS: a Melting Model for the Martian Mantle and FeO-rich Peridotite. *Journal of Geophysical Research: Planets* <https://doi.org/10.1029/2021JE006985>
- [2] McSween, H. Y., Wyatt, M. B., Gellert, R., et al. (2006). Characterization and petrologic interpretation of olivine-rich basalts at Gusev Crater, Mars. *Journal of Geophysical Research E: Planets*, 111(2), 1–17. <https://doi.org/10.1029/2005JE002477>
- [3] Monders, A. G., Médard, E., & Grove, T. L. (2007). Phase equilibrium investigations of the Adirondack class basalts from the Gusev plains, Gusev crater, Mars. *Meteoritics and Planetary Science*, 42(1), 131–148. <https://doi.org/10.1111/j.1945-5100.2007.tb00222.x>
- [4] Filiberto, J., Treiman, A. H., & Le, L. (2008). Crystallization experiments on a Gusev Adirondack basalt composition. *Meteoritics and Planetary Science*, 43(7), 1137–1146.
- [5] Kinzler, R. J., & Grove, T. L. (1992). Primary magmas of mid-ocean ridge basalts 1. Experiments and methods. *Journal of Geophysical Research*, 97(B5), 6885–6906. <https://doi.org/10.1029/91JB02840>
- [6] Collinet, M., Médard, E., Charlier, B., Vander Auwera, J., & Grove, T. L. (2015). Melting of the primitive martian mantle at 0.5–2.2 GPa and the origin of basalts and alkaline rocks on Mars. *Earth and Planetary Science Letters*, 427, 83–94. <https://doi.org/10.1016/j.epsl.2015.06.056>
- [7] Bertka, C. M., & Holloway, J. R. (1994). Anhydrous partial melting of an iron-rich mantle II: primary melt compositions at 15 kbar. *Contributions to Mineralogy and Petrology*, 115(3), 323–338. <https://doi.org/10.1007/BF00310771>
- [8] Agee, C. B., & Draper, D. S. (2004). Experimental constraints on the origin of Martian meteorites and the composition of the Martian mantle. *Earth and Planetary Science Letters*, 224(3–4), 415–429. <https://doi.org/10.1016/j.epsl.2004.05.022>
- [9] Matsukage, K. N., Nagayo, Y., Whitaker, M. L., Takahashi, E., & Kawasaki, T. (2013). Melting of the Martian mantle from 1.0 to 4.5 GPa. *Journal of Mineralogical and Petrological Sciences*, 108(4), 201–214. <https://doi.org/10.2465/jmps.120820>
- [10] Ghiorso, M. S., Hirschmann, M. M., Reiners, P. W., & Kress, V. C. (2002). The pMELTS: A revision of MELTS for improved calculation of phase relations and major element partitioning related to partial melting of the mantle to 3 GPa. *Geochemistry, Geophysics, Geosystems*, 3(5), 1–35. <https://doi.org/10.1029/2001gc000217>
- [11] Connolly, J. A. D. (2009). The geodynamic equation of state: What and how. *Geochemistry, Geophysics, Geosystems*, 10(10). <https://doi.org/10.1029/2009GC002540>

- [12] Holland, T. J. B., Green, E. C. R., & Powell, R. (2018). Melting of Peridotites through to Granites: A Simple Thermodynamic Model in the System KNCFMASHTOCr. *Journal of Petrology*, 59(5), 881–900. <https://doi.org/10.1093/petrology/egy048>
- [13] Santos, A. R., Agee, C. B., McCubbin, F. M., Shearer, C. K., Burger, P. V., Tartèse, R., & Anand, M. (2015). Petrology of igneous clasts in Northwest Africa 7034: Implications for the petrologic diversity of the martian crust. *Geochimica et Cosmochimica Acta*, 157(0), 56–85. <https://doi.org/10.1016/j.gca.2015.02.023>
- [14] Musselwhite, D. S., Dalton, H. A., Kiefer, W. S., & Treiman, A. H. (2006). Experimental petrology of the basaltic shergottite Yamato-980459: Implications for the thermal structure of the Martian mantle. *Meteoritics and Planetary Science*, 41(9), 1271–1290. <https://doi.org/10.1111/j.1945-5100.2006.tb00521.x>
- [15] Udry, A., Lunning, N. G., McSween Jr, H. Y., & Bodnar, R. J. (2014). Petrogenesis of a vitrophyre in the martian meteorite breccia NWA 7034. *Geochimica et Cosmochimica Acta*, 141(0), 281–293. <https://doi.org/http://dx.doi.org/10.1016/j.gca.2014.06.026>
- [16] He, Q., Xiao, L., Hsu, W., Balta, J. B., McSween, H. Y., & Liu, Y. (2013). The water content and parental magma of the second chassignite NWA 2737: Clues from trapped melt inclusions in olivine. *Meteoritics and Planetary Science*, 48(3), 474–492. <https://doi.org/10.1111/maps.12073>
- [17] Collinet, M., Charlier, B., Namur, O., Oeser, M., Médard, E., & Weyer, S. (2017). Crystallization history of enriched shergottites from Fe and Mg isotope fractionation in olivine megacrysts. *Geochimica et Cosmochimica Acta*, 207, 277–297. <https://doi.org/10.1016/j.gca.2017.03.029>
- [18] Basu Sarbadhikari, A., Day, J. M. D., Liu, Y., Rumble, D., & Taylor, L. a. (2009). Petrogenesis of olivine-phyric shergottite Larkman Nunatak 06319: Implications for enriched components in martian basalts. *Geochimica et Cosmochimica Acta*, 73(7), 2190–2214. <https://doi.org/10.1016/j.gca.2009.01.012>
- [19] Lodders, K., & Fegley, B. (1997). An oxygen isotope model for the composition of Mars. *Icarus*, 126(2), 373–394. <https://doi.org/10.1006/icar.1996.5653>
- [20] Dreibus, G., & Wänke, H. (1985). Mars, a volatile-rich planet. *Meteoritics*, 20(2), 367–381.
- [21] Yoshizaki, T., & McDonough, W. F. (2020). The composition of Mars. *Geochimica et Cosmochimica Acta*, 273, 137–162. <https://doi.org/10.1016/j.gca.2020.01.011>
- [22] Knapmeyer-Endrun, B., Panning, M. P., Bissig, F., et al. (2021). Thickness and structure of the martian crust from InSight seismic data. *Science*, 373(6553), 438–443. <https://doi.org/10.1126/science.abf8966>

